

## Comparison of Kinematics of GHBMCM to PMHS on the Side Impact Condition

Gwansik Park, Taewung Kim, Jeff R. Crandall, Carlos Arregui-Dalmases, Javier Luzon-Narro

**Abstract** The goal of this study was to evaluate the biofidelity of the Global Human Body Models Consortium (GHBMCM) human body model under a side impact loading condition with an airbag, and analyze the effect of initial position of the model on the response. Shaw et al. conducted side impact sled tests using three Post mortem human surrogates (PMHS) with impact speeds of  $4.3 \pm 0.1$  m/s, and used a rigid wall boundary condition with an airbag mounted to the sled. The correlation between the PMHS and the GHBMCM was evaluated using the CORA rating method. The rating ranged from 0.27 to 0.69 along the body regions on a scale in which a rating of 1.0 indicated a perfect correlation between the PMHS and the GHBMCM. The pelvis and thorax region showed good correlation with those of the PMHS while the spinal regions did not. In addition, the roll and yaw angle of the initial position of the PMHS had an effect on the response of subjects. The result of this research indicated two points, that the GHBMCM model should be validated focusing on the internal biofidelity of the model, and that the yaw and roll angle should be carefully controlled during a side impact test.

**Keywords** Biofidelity, GHBMCM, Kinematics, Side impact

### I. INTRODUCTION

In the field of biomechanics, post mortem human surrogates (PMHS), volunteers, anthropometric test devices (ATDs), animals and computational models have been employed to quantify the response and injury tolerance of a live human [1]. With the recent development of computational technology and software, the use of full human body finite element (FE) models have been expanded for over a decade. Two models have been widely used in the field: The Human Model for Safety (HUMOS) [4] and Total Human Model for Safety (THUMS) [5]-[7].

The main advantage of the full human body FE model is its capability to predict injuries based on local values of stress and strain, offering considerable advantages over simpler multi-body models, dummies, and in some circumstances even PMHS. However, the accuracy of any computational model for the assessment of injury risk depends inherently on the quality of the model in terms of model geometry and material properties [1]. Thus, the biofidelity of the human FE model should be evaluated across various loading conditions.

The male 50th percentile GHBMCM model has been developed by Global Human Body Models Consortium<sup>TM</sup> and validated from the component level to whole body sled test responses [19]-[25]. The biofidelity of this model was also evaluated in lateral sled tests and drop test conditions, focusing on the impact force, thorax deflection and rib fracture [18]. The kinematics of bony structures including the head, spine, and pelvis have not been evaluated. However, differences in body kinematics affect the forces and accelerations that occur in the spine and thorax [8]. Shaw et al. conducted PMHS sled tests in which significant information about the occupant response was measured, including kinematics of body regions [9], which may provide an ideal basis to assess the biofidelity of the computational models in predicting human response and injury.

The goal of this study was to compare the responses of the GHBMCM model under the side impact condition to that of the PMHS, not only the impact forces from the impact wall but also the kinematics. The level of validation was evaluated objectively using a correlation analysis. The effects of varying the initial position on response of the human body model were analyzed using a sensitivity analysis.

G. Park is a graduate student (tel: +1 (434) 296-7288, fax: +1 (434) 296-3453, [gp6xr@virginia.edu](mailto:gp6xr@virginia.edu)), T. Kim is a research scientist and J.R. Crandall is Professor at the University of Virginia Center for Applied Biomechanics, Charlottesville, Virginia. C. Arregui-Dalmases is a visiting assistant professor at the University of Virginia and an associate professor at the Universitat Politècnica de Catalunya (UPC) Barcelona Tech. J. Luzon-Narro is an associate professor at the Universitat Politècnica de Catalunya (UPC) Barcelona Tech.

## II. METHODS

To evaluate the biofidelity of the GHBM model to the PMHS, two methods were employed: correlation analysis (CORA) and analysis of variance (ANOVA). The correlation analysis objectively assessed the reliability of the model and the ANOVA analyzed the effect of the initial position variance of the human body model on its response. The experimental testing data using the PMHS in this research was based on previous work conducted by Shaw et al. [9]. A brief description of their test set-up was provided in this paper, while more complete details of the test set-up can be found in Shaw et al. [9]: Three approximately 50<sup>th</sup> percentile adult male PMHS were used for testing (test 1569, test 1570, and test 1571) and each subject had different anthropometry. In this study, test1570 (stature: 175cm) was selected as the reference data due to its similar stature to the GHBM model. LS-DYNA double precision MPP R4.2.1 was used for the simulations.

### **Test Fixtures**

The right side of PMHS was struck at  $4.3 \pm 0.1$  m/s by a rigid wall with the side airbag on a sled. There were fifteen separate load cell plates supported by a load cell in the wall buck and they were distributed from the head to lower extremity regions (Figure 3). The seat was inclined 15 degrees backward without a backrest, and a foam pad was placed between the distal thighs and the seat to achieve a target femur angle. Both the top and bottom of the seat was covered with Teflon to create a coefficient of friction of 0.249. In this study, the FE model of load cell wall and seat cushion were assumed to be a rigid body.

### **GHBM Model**

The GHBM male 50<sup>th</sup> percentile model (version: FMB v.3-5, weight: 77.1 kg, and height: 175.3 cm) [19]-[25] was used in this study. Overall, this FE human model consists of 1.3 million nodes, 1.95 million elements, and 847 parts. The fracture of bone was modeled by using effective failure strain. If an element reached the failure strain, then the element was deleted. Shaw et al. amputated the forearms of their PMHS to improve visibility during motion tracking [9]. Therefore, the forearms of the human model were removed, and nodes in cutting plane were defined as rigid bodies by using the \*CONSTRAINED \_NODAL\_RIGID\_BODY keyword in LS-DYNA (Figure 1) [10].

### **Side Airbag**

During the side impact tests a custom large volume, dual inflator side airbag was deployed prior to contact with the subject's thorax timing that allowed for full inflation prior to thorax loading. The airbag was mounted using a hinge with a rotational spring (Figure 3). The rotational joint of the mounting system was modeled using a connector element. The FE side airbag model was modeled using an \*Airbag\_Hybrid model which was supported in LS-DYNA [10]. This was a simple way to model the airbag assuming uniform pressure without flow direction. The airbag deployed as shown in Figure 3. The side airbag model was validated by a previous research that compared the impact forces and lateral accelerations of the ES-2re FE model to that of the ES-2re dummy in the test [14].

### **Data Processing**

The accelerations of the head, T1, T6, T11, L3 and pelvis were obtained using a tri-axial accelerometer. The kinematics of PMHS were determined using a VICON<sup>TM</sup> motion capture camera system. Using the VICON<sup>TM</sup> system 3-dimensional motions of the anatomical structures were captured through a transformation of a marker-based coordinate system to the anatomical coordinate system [9]. In this study, the lateral acceleration of T1, T6, and pelvis and the kinematics of spine of the GHBM model were compared to those of the reference PMHS. During the tests, two dimensional torso deformation was measured using a chestband [12], which encircled the torso at the level of the sixth rib laterally. The central thorax deflection from the chestband (distance between point B and point E) was compared to assess the chest deflection (Figure 2).

To compensate the different anthropometries of the cadaver and GHBM human model, the responses of the cadaver were scaled to the standard anthropometry of the 50th percentile male, which is the same with the GHBM model, by using a mass scaling technique proposed by Eppinger et al. [28]

In the GHBM model, impact forces were taken by contact force between the wall buck and the subject and the acceleration was obtained. The nodal velocity output was differentiated to obtain acceleration time histories at T1, T6, and pelvis because the GHBM model (v3.5) did not used acceleration elements at the locations of interest and the nodal acceleration data was very noisy even after filtering. Chest deflection was

calculated by measuring the distance between two center nodes in the chestband and normalized using the initial distance between two nodes in the GHBM model.

All the data were represented according to SAE J1733 [16]. The coordinates system used in this study is shown in Figure 3. For the comparison between the response of the PMHS and the human model, the impact forces and accelerations were filtered using the CFC180 [17].

### **Initial Position**

There was variation in the initial position of the subjects during testing due to the subjects themselves and the tether support system. Although the target position during the PMHS tests were the UMTRI driving position [11] which the GHBM model was developed to target it, the initial position variance needed to be checked to ensure similar test conditions. The initial position of the PMHS was compared using the position data from the VICON markers in the test (Figure 4).

### **Correlation Analysis**

The objective evaluation of the level of correlation of the GHBM responses and a reference PMHS was analyzed using the correlation and analysis method (CORA) [15]. The rating of each response was calculated and overall rating of the model was obtained by averaging all the responses with same weight factor. The CORA parameters used in this study is shown in Table I. Since the CORA rating score is a relative measure to understand the meaning of the CORA rating score between responses of the GHBM model and the reference PMHS, CORA rating scores calculated between responses of the reference PMHS (test 1570) and other PMHSs (test 1569 and test 1571).

### **Sensitivity Analysis**

To analyze the effect of initial position to the subject responses, a one-half fraction of two-level factorial design of experiment was used for the sensitivity analysis of initial positions of the GHBM model on its responses. Five variables, which were vertical position, horizontal position, pitch angle, roll angle, and yaw angle, and seven responses, which were shoulder, thorax, and pelvis impact force, T1, T6, and pelvis accelerations, and chest compression, were considered for the sensitivity analysis. Since the responses were time histories not only peak values and timing of those but also CORA ratings were used for the sensitivity analysis to evaluate overall correlation between a pair of signals.

Eight anatomical locations of cadavers were measured by using Vicon™ camera systems as shown in Figure 4 (left). Vertical and horizontal positions were defined based on the location of the pelvis marker. The roll and pitch were calculated by measuring angles between the vector from the pelvis to the T1 and the projected vectors of it on the xz-plane and yz-plane, respectively. The yaw angle was calculated by measuring angle between the vector from the pelvis to the mid-point of left and right patellas and the projected vector of it on the xy-plane.

To determine the levels of the five design variables, the initial position data of three PMHS (test 1413, test 1414, and test 1415) [13] were additionally used with those from the study of Shaw et al. [9] to increase the number of PMHSs. Tests performed by Lessely et al. [13] were similar to those of Shaw et al., except a rigid wall condition was used instead of an airbag condition. One standard deviations of each design variables were used as levels and UMTRI driving position was used as a baseline position because this position was the target for PMHS tests (Table II). Since the GHBM model has been developed targeting the UMTRI sitting posture as initial posture, the model was selected as the baseline model for sensitivity analysis. In addition to the baseline model, which was used for comparing the responses to PMHS responses, sixteen more simulations were performed by imposing the initial position errors for the sensitivity analysis. The whole GHBM model was translated and rotated with respect to its pre-defined origin (Figure 1). Also the upper surface of seat foam was rotated together with the GHBM model for the pitch and roll rotation. The rotations of the GHBM model were applied in the order of yaw, pitch and roll angle.

Sensitivity of the initial position on the responses of the GHBM model were analyzed through ANOVA analysis. The normality of residuals of three measures, which were peak value, peak time, and CORA rating, of the seven responses of the GHBM model were tested by using the Anderson-Darling normality test. ANOVA analysis was performed only for the measures whose residuals showed normality. Also, main effects of the design variables were analyzed to evaluate the magnitude of changes in responses due to the initial positions.

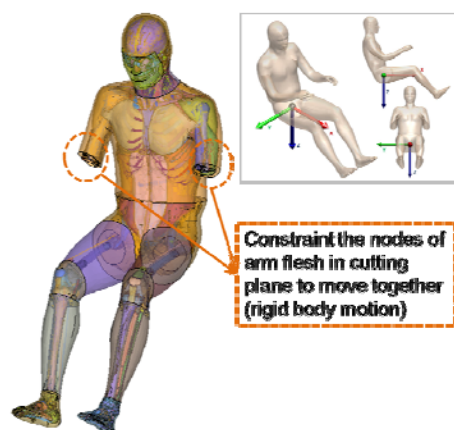


Fig. 1. Forearm elements removed GHBM (FBM v3.5) model and origin of the model

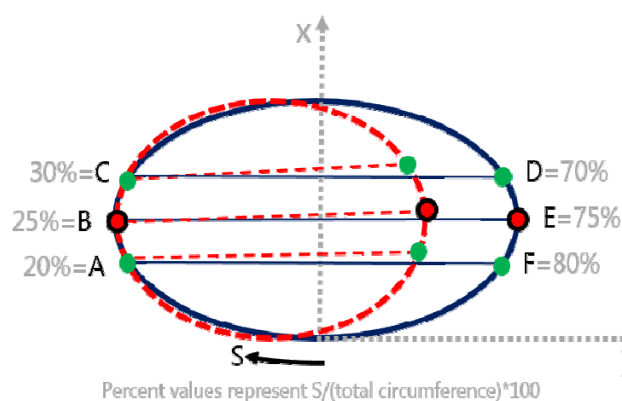


Fig. 2. Full thorax deflection using the chestband

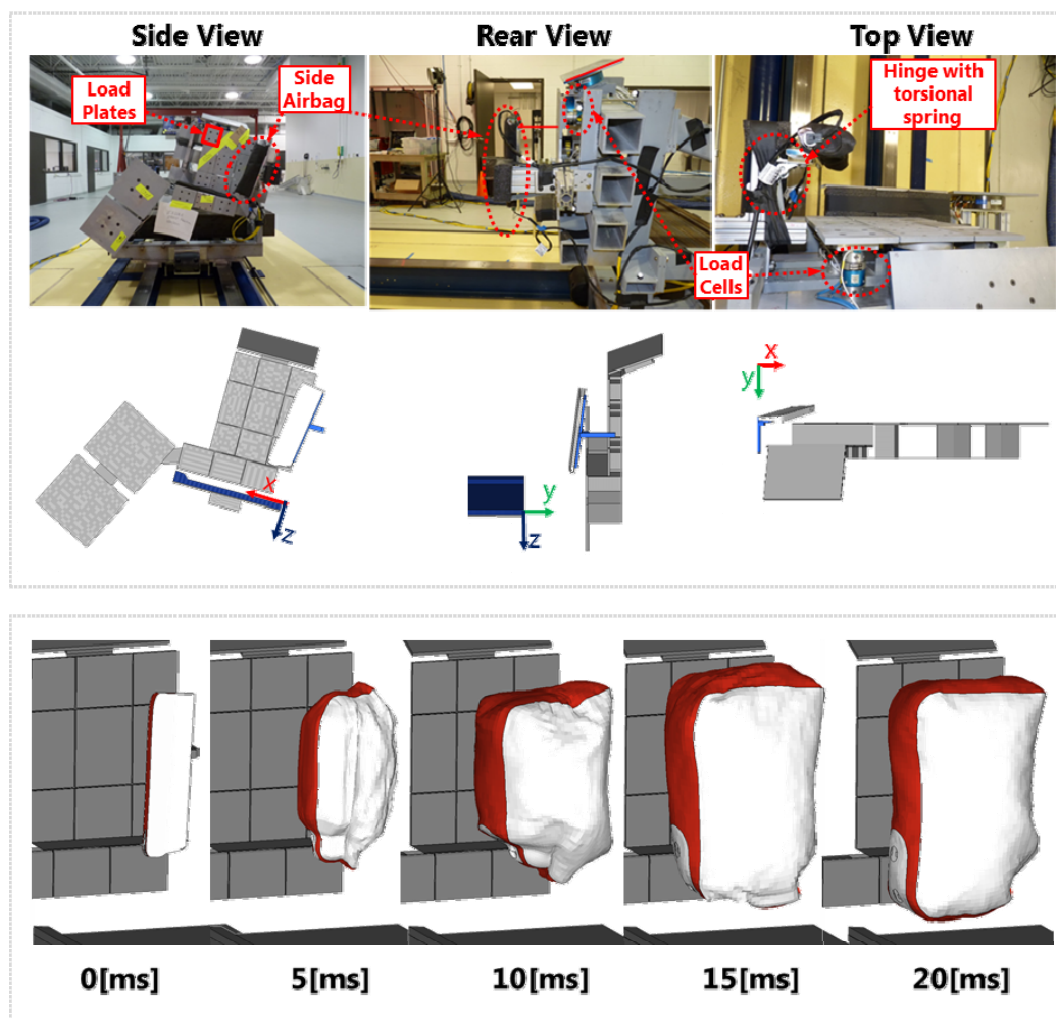


Fig. 3. Wall buck with load cell with side airbag mounting system and coordinates system (upper) and sequences of deployment of the side airbag (below)

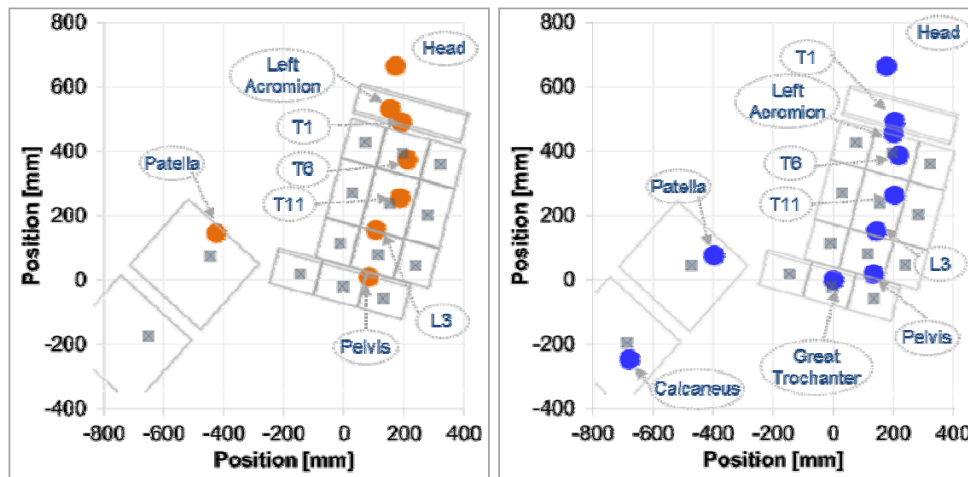


Fig. 4. Comparison of Initial position at the anatomical landmarks from the VICON data between test 1570 (left) and the GHBM model (right)

TABLE I  
CORA parameters used in this research

A_THRES	B_THRES	A_EVAL	B_DELTA_END	K	G_1
0.030	0.075	0.010	0.200	2	0.5
a_0/b_0	a,b_sigma	D_MIN	D_MAX	INT_MIN	K_V
0.05	0	0.01	0.12	0.80	10
K_G	K_P	G_V	G_G	G_P	G_2
1	1	0.50	0.25	0.25	0.50

TABLE II  
Initial position variance of six PMHS

Variables	(+) Direction	test 1569	test 1570	test 1571	test 1413	test 1414	test 1415	STD
Vertical [mm] (along Z-axis)		178	183	199	149	162	183	18
Horizontal [mm] (along X-axis)		-59	-51	-92	11	-3	11	43
Pitch Angle [deg] (along Y-axis)		5	2	-3	4	-1	-5	4
Roll Angle [deg] (along X-axis)		-7	4	3	4	0	-8	5
Yaw Angle [deg] (along Z-axis)		-2	0	1	-4	-2	-1	2

### III. RESULTS

The responses of the GHBM human body model was compared to the reference PMHS (test 1570) responses as shown in Figure 5, Figure 6, and Figure 7. The shoulder of GHBM model sustained higher peak impact force than the PMHS and showed higher T1 and T6 Y-axis peak acceleration than those of the PMHS responses. Also, GHBM showed stiffer responses than the PMHS in terms of the chest compression. This correlation can be well explained in Table III, which consists of peak values for each response, its peak time and the CORA rating, which implies the level of correlation objectively. The CORA rating of the GHBM human body model ranged from 0.27 to 0.69 for the each response and the overall rating was 0.53 using the average of all the responses. Additionally, the kinematics of bony structures around the spine were compared between the GHBM model and the PMHS (Figure 8). The GHBM position along the Y-axis seems similar to that of PMHS, however, the location of pelvis in the GHBM human body model remained stayed along the z-axis while the PMHS pelvis was going up along the z-axis.

The sensitivity analysis results of seventeen cases including peak value, peak time and CORA rating are

summarized in Table IV. Using the result in Table IV., ANOVA was performed to find the most influential variables on the responses of the model and the results were summarized in Table V. From the ANOVA results, the variation of the roll angle affected the most number of responses and showed statistically significant ( $p < 0.05$ ) effect on the peak impact force at the shoulder and its timing, the peak impact force of thorax, the peak Y-axis acceleration and its time of T1 and T6. The horizontal direction had a significant effect ( $p < 0.05$ ) on the peak impact force of thorax and peak Y-axis acceleration of T1. Furthermore, the variation of the yaw angle significantly ( $p < 0.05$ ) affected, peak impact force and Y-axis acceleration of the pelvis. Main effect of the design variables on the peak values were shown in Figure 9.

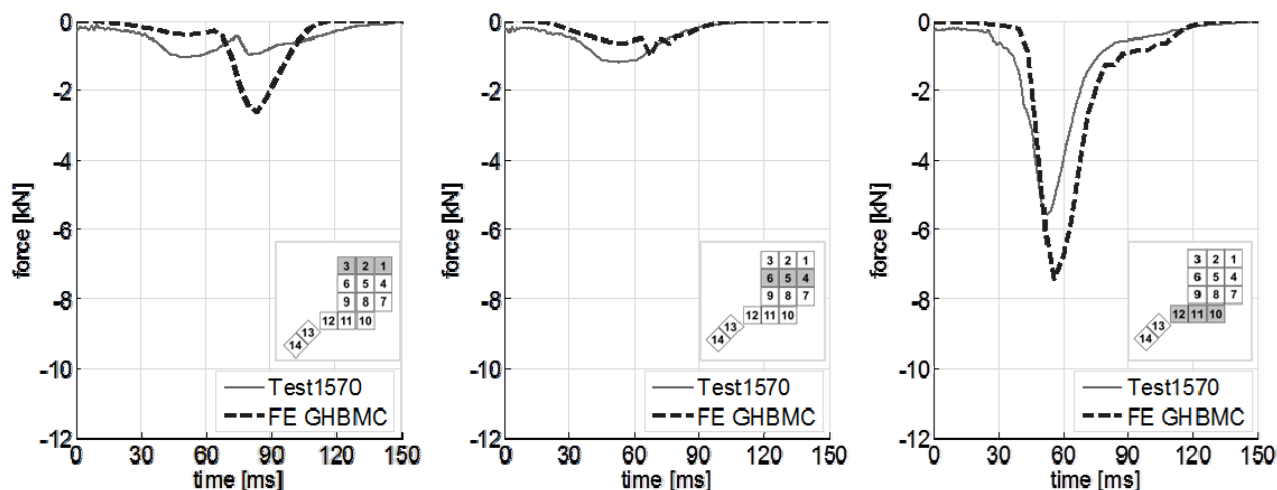


Fig. 5. Comparison of impact force time history : shoulder (left), thorax (middle), pelvis (right)

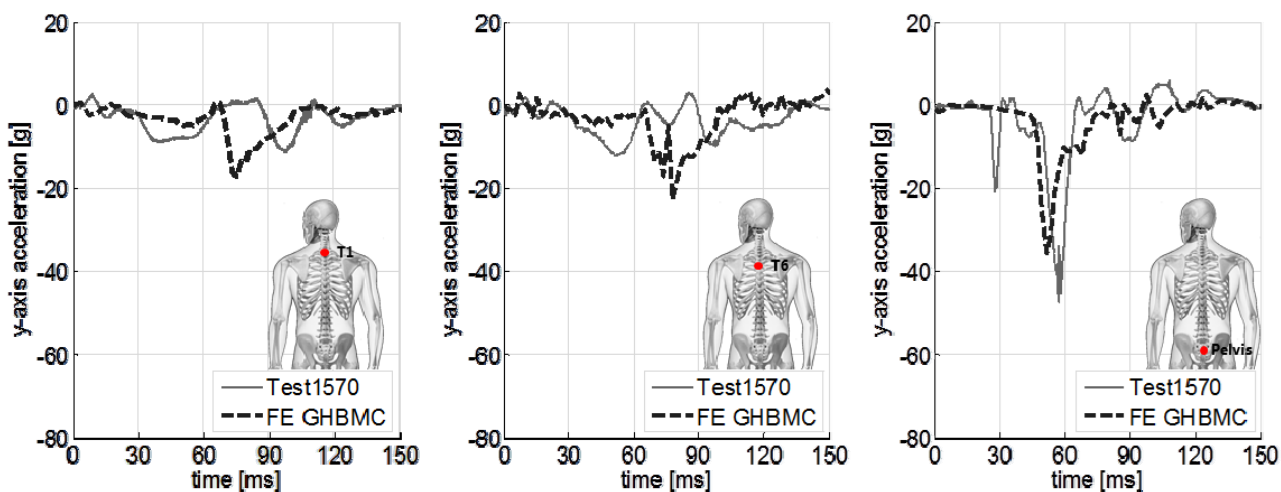


Fig. 6. Comparison of Y-axis acceleration time history: T1 (left), T6 (middle), pelvis (right)

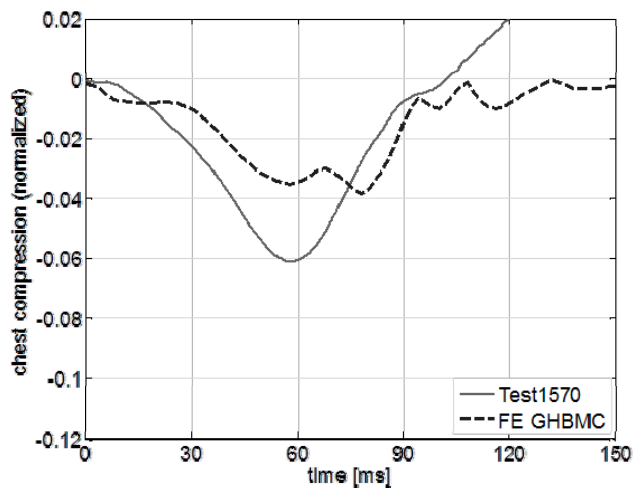


Fig. 7. Comparison of chest compression time history

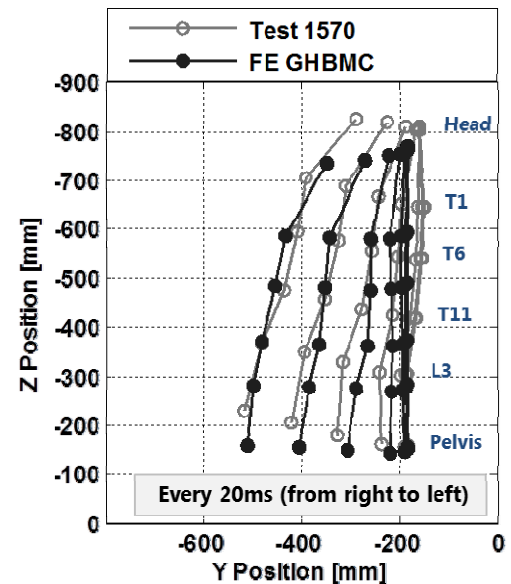


Fig. 8. Spinal position from 0 – 120 ms with respect to the seat coordinate system

TABLE III  
Summary of biofidelity evaluation results

Subject		Impact Force [kN]			Y axis acc. [g]			Chest Deflection [%]	Average CORA Rating
		Shoulder	Thorax	Pelvis	T1	T6	Pelvis		
Test 1570	Peak value	1.02	1.18	5.55	11	12	42	6.10	
	Peak Time [ms]	51	53	52	97	51	57	57	
Test 1569	Peak value	1.38	0.83	7.06	15	13	41	2.94	0.57
	Peak Time [ms]	104	65	49	95	100	54	65	
	COAR Rating	0.41	0.68	0.85	0.58	0.39	0.72	0.35	
Test 1571	Peak value	1.19	1.31	6.17	12	12	36	6.56	0.63
	Peak Time [ms]	102	65	52	104	57	60	70	
	COAR Rating	0.53	0.69	0.78	0.62	0.60	0.74	0.46	
GHBM	Peak value	2.62	1.25	7.43	18	23	36	4.25	0.53
	Peak Time [ms]	84	65	56	75	77	52	99	
	COAR Rating	0.44	0.69	0.67	0.37	0.27	0.68	0.57	

TABLE IV  
Summary of data

No.	Ver. [mm]	Hor. [mm]	Pitch [deg]	Roll [deg]	Yaw [deg]	Peak	Impact Force [kN]			Y acc. [g]			Chest Def. [%]	Ave. Rating
							Sho.	Tho.	Pelvis	T1	T6	Pelvis		
1	-18	-43	-4	-5	2	Value	-1.89	-1.22	-7.14	-16	-19	-32	5.18	0.71
						Time	96	73	105	91	87	56	100	
						Rating	0.64	0.73	0.77	0.59	0.67	0.78	0.80	
2	18	-43	-4	-5	-2	Value	-1.58	-1.18	-8.10	-13	-13	-34	5.92	0.76
						Time	97	53	56	91	98	51	100	
						Rating	0.62	0.73	0.93	0.58	0.65	0.95	0.83	
3	-18	43	-4	-5	-2	Value	-2.74	-1.35	-7.90	-20	-23	-41	6.02	0.79
						Time	85	62	57	79	87	53	103	
						Rating	0.85	0.68	0.88	0.70	0.77	0.88	0.75	
4	18	43	-4	-5	2	Value	-2.27	-1.46	-7.05	-18	-20	-31	5.57	0.75
						Time	88	61	57	80	84	53	101	
						Rating	0.80	0.57	0.97	0.62	0.70	0.85	0.76	
5	-18	-43	4	-5	-2	Value	-1.58	-1.18	-8.07	-14	-14	-37	6.31	0.71
						Time	99	53	57	94	102	55	103	
						Rating	0.60	0.71	0.91	0.44	0.62	0.85	0.80	

6	18	-43	4	-5	2	Value	-1.58	-1.18	-6.60	-14	-14	-29	6.13	
						Time	99	53	58	94	102	53	103	0.68
						Rating	0.40	0.71	0.90	0.42	0.63	0.87	0.83	
7	-18	43	4	-5	2	Value	-2.31	-1.33	-7.04	-23	-21	-38	5.23	
						Time	88	66	57	89	93	55	103	0.78
						Rating	0.68	0.87	0.93	0.64	0.71	0.84	0.81	
8	18	43	4	-5	-2	Value	-1.73	-1.23	-7.90	-16	-20	-42	5.56	
						Time	91	69	56	90	82	55	102	0.76
						Rating	0.66	0.74	0.91	0.62	0.70	0.88	0.78	
9	-18	-43	-4	5	-2	Value	-3.20	-1.20	-8.16	-27	-22	-30	4.10	
						Time	72	63	56	62	75	56	77	0.73
						Rating	0.59	0.71	0.96	0.58	0.69	0.88	0.70	
10	18	-43	-4	5	2	Value	-2.74	-1.63	-6.74	-21	-22	-29	3.65	
						Time	78	65	59	68	78	56	73	0.83
						Rating	0.74	0.90	0.89	0.76	0.81	0.87	0.82	
11	-18	43	-4	5	2	Value	-4.16	-1.61	-7.08	-38	-28	-33	3.66	
						Time	68	48	58	57	61	50	85	0.69
						Rating	0.51	0.66	0.98	0.47	0.56	0.86	0.83	
12	18	43	-4	5	-2	Value	-3.37	-1.93	-8.23	-39	-25	-32	3.41	
						Time	67	51	58	59	64	54	87	0.67
						Rating	0.54	0.62	0.74	0.49	0.58	0.86	0.82	
13	-18	-43	4	5	2	Value	-2.69	-1.18	-6.71	-21	-21	-26	3.81	
						Time	79	53	56	69	75	53	71	0.79
						Rating	0.76	0.67	0.93	0.79	0.79	0.85	0.75	
14	18	-43	4	5	-2	Value	-2.29	-1.24	-8.74	-17	-19	-32	3.95	
						Time	81	72	58	71	76	53	74	0.82
						Rating	0.84	0.81	0.81	0.82	0.80	0.86	0.79	
15	-18	43	4	5	-2	Value	-3.48	-1.69	-8.20	-29	-28	-33	3.82	
						Time	68	54	58	60	69	52	76	0.70
						Rating	0.54	0.69	0.80	0.55	0.64	0.87	0.78	
16	18	43	4	5	2	Value	-3.04	-1.58	-9.03	-28	-27	-29	3.24	
						Time	69	55	59	63	70	51	76	0.73
						Rating	0.60	0.73	0.85	0.57	0.65	0.88	0.85	

\* Abbreviations : Vertical (Ver.), Horizontal(Hor.), Shoulder (Sho.), Thorax (Tho.)

TABLE V.  
Sensitivity analysis results : significant effect variables using the analysis of variance (ANOVA)

Category		Normality (p > 0.05)	Effectiveness (p < 0.05)				
			Ver.	Hor.	Pitch	Roll	Yaw
Shoulder Impact Force	Peak value	0.89	0.22	0.06	0.24	0.00	0.89
	Peak time	0.25	0.76	0.10	0.63	0.00	0.90
	CORA	0.84	0.97	1.00	0.68	0.79	0.81
Thorax Impact Force	Peak value	0.80	0.67	0.01	0.21	0.05	0.87
	Peak time	0.09	0.89	0.64	0.93	0.37	0.95
	CORA	0.14	0.79	0.21	0.37	0.93	0.70
Pelvis Impact Force	Peak value	0.10	0.52	0.51	0.54	0.32	0.00
	Peak time	0.01	-	-	-	-	-
	CORA	0.23	0.60	0.90	0.80	0.38	0.35
T1 Y axis Acc.	Peak value	0.34	0.44	0.03	0.31	0.00	0.94
	Peak time	0.06	0.80	0.26	0.46	0.00	0.95
	CORA	0.62	0.80	0.50	0.88	0.42	0.86
T6 Y axis Acc.	Peak value	0.25	0.78	0.08	0.19	0.04	0.98
	Peak time	0.79	0.93	0.10	0.53	0.00	0.95
	CORA	0.46	0.85	0.27	0.77	0.81	0.89
Pelvis	Peak value	0.17	0.46	0.11	0.88	0.03	0.04

Y axis Acc.	Peak time	0.46	0.71	0.20	0.79	0.50	0.86
	CORA	0.01	-	-	-	-	-
Chest Compression	Peak value	0.03	-	-	-	-	-
	Peak time	0.01	-	-	-	-	-
	CORA	0.39	0.11	0.79	0.65	0.88	0.23

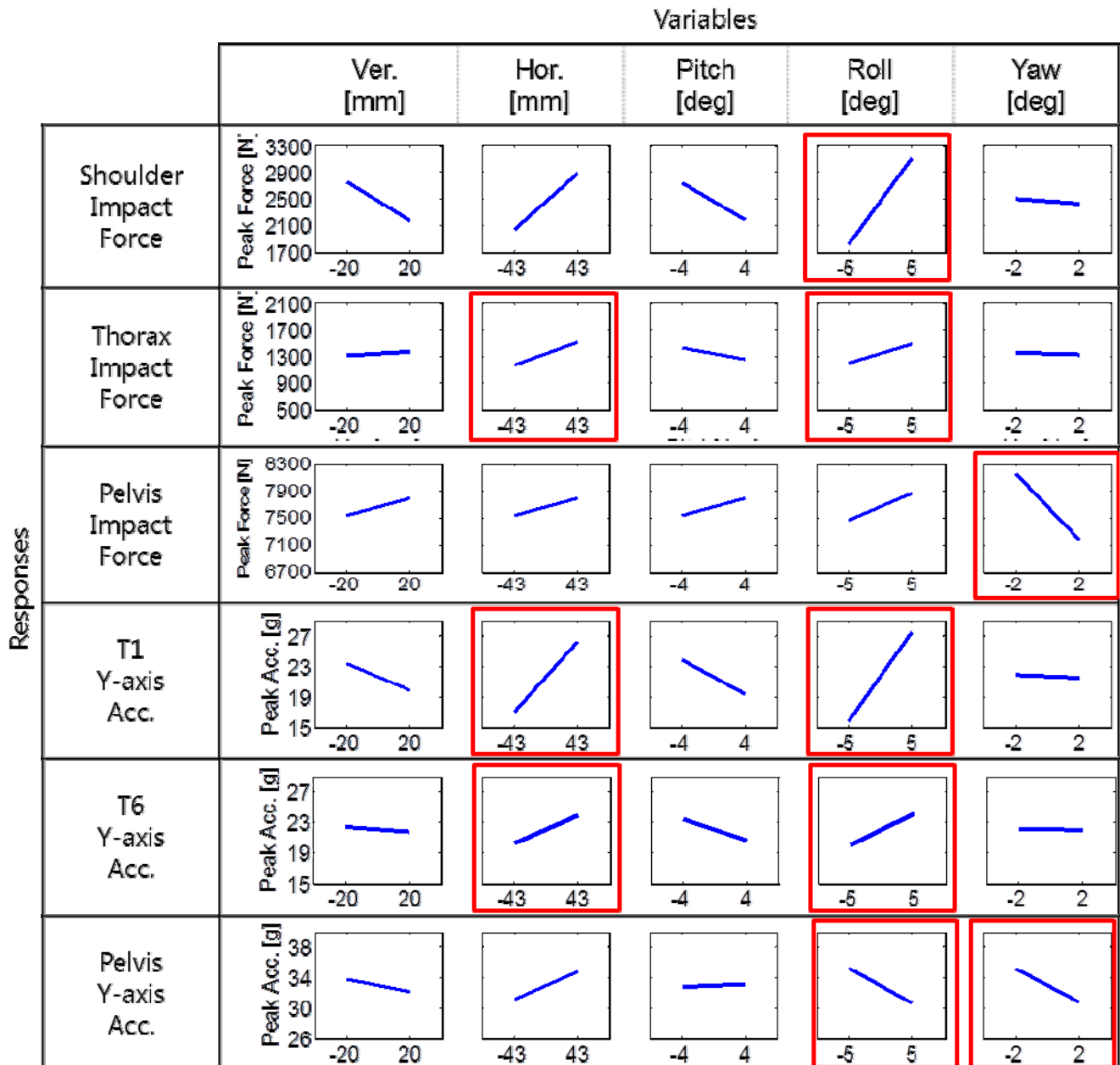


Fig. 9. Main Effect Plot using the peak value of variables

#### IV. DISCUSSION

##### *Evaluating the Biofidelity (Impact forces and Kinematics) using Correlation Analysis*

The results showed relatively poor correlation at the shoulder region of subjects. The error might come from the interaction between the airbag and the shoulder region. Since the shoulder was located almost at the edge of the airbag, the geometric differences of the subjects highly influences to the response. In other words, the shoulder of some subjects were exposed to the rigid wall while the others were covered by the airbag during the test.

The GHBMC human body model showed the best validation results at the thorax region in terms of impact

force by comparing the CORA rating to that of PMHS's as shown in Table III. Despite good correlation of test1569 and test 1571 for thorax response to the target PMHS response, chest deflection indicated relatively poor correlation. This might indicate that the internal biofidelity of the thorax region highly depends on the material property. The pelvis region of the GHBMC model showed relatively high rating, however, it is still lower rating than the PMHS's. The GHBMC model showed the lowest rating at the spinal (T1,T6) region among other responses. This may be a result of the compliance of the GHBMC model. Based upon the impact force distribution, which showed good correlation with the test data, this problem may have resulted from the GHBMC model. This implies that the GHBMC model is not good enough to investigate injury risk in stress-strain levels because it could not capture the localized deformation modes seen in the PMHS.

Although the responses were scaled based on the mass ratio and the 50<sup>th</sup> percentile male PMHS that were selected for this study, there were still differences in terms of anthropometry. Also, the target PMHS had scoliosis as shown in Figure 8; the initial spinal points of the reference PMHS were located closer to the wall buck than the head and pelvis, but the GHBMC had straight spine in its sagittal plane. Another source of the difference could be modeling error of the GHBMC. For instance, thoracic and lumbar vertebrae of the GHBMC model were assumed as rigid bodies, and this may have contributed to the stiffer responses of the model. Furthermore, the types of elements of the disk parts on the lumbar and thoracic region were different, and it is not clear whether a disk could be modeled by only using shell elements. Lastly, the airbag model was validated based on a dummy test data [14], but there could be discrepancy between the FE model and the real product.

### ***Effect of Initial position variables on the response (Analysis of Variance)***

As shown in Table IV, the initial sitting position variation of roll angle had the most number of significant effects on the responses. This may have been a result of differences in impact timing of each body region due to the roll rotation. The total energy from the impact was the same regardless of the angle variation, therefore increasing impact force at one body region decreased the force at other body regions. For instance, a plus roll angle decreased the shoulder distance from the wall and increased the load of the shoulder region. The pelvis impact force decreased due to the increased shoulder impact force.

The mechanism which was applied to the roll angle may have influenced the yaw angle due to the dependency of pelvis and lower extremity region. Because the pelvis region was coupled with the lower extremity region, impact timing of each body region made response different and this was reflected the significant effect of yaw angle on the pelvis responses.

The variation of pitch angle does not affect the responses because it does not change the impact timing of each body region. The horizontal directional variance affected the peak impact force on the thorax and Y-axis acceleration of T1. It might be due to the interaction between the airbag and the thorax. In other words, the thorax region was first impacted by the airbag and the location of impact was determined by the initial position of the subject.

It is noted that variables using the CORA rating did not have any significant effect on the responses. Although the rating method could consider the whole time history of the response including peak value as well as peak time, however, it may not be a good measure for the sensitivity analysis because the CORA rating cannot consider signs in measuring differences. It treats responses the same whether they are a certain amount higher or lower than a target response. Since baseline is at the middle of responses generated by changing design variables for a sensitivity analysis, it is expected that CORA cannot capture the main effects of those variables well.

## **V. CONCLUSIONS**

The biofidelity of the 50th percentile male GHBMC model and the sensitivity of the initial positions on its responses were evaluated under a side impact loading conditions with a side airbag. It can be concluded from the results that

1. The GHBMC model showed good correlations in pelvis wall load and accelerations with those of PMHS.
2. However, the shoulder area of the GHBMC model is needed to be improved because it showed higher wall load and T1 acceleration than those of PMHS.
3. It is difficult to evaluate the biofidelity of the thorax area because this body region was not highly engaged during the side impact event.
4. The external biofidelity of the GHBMC in terms of impact force showed better correlations (rating = 0.60)

with those of the PMHS than the internal biofidelity of the GHBMC model (lateral accelerations of components and chest deflection, rating = 0.47). It implies that the GHBMC model should be further validated focusing on the internal biofidelity.

5. The results of the sensitivity analysis of the initial position suggest that the initial roll and yaw angles of a surrogate should be controlled carefully during a side impact test.
6. CORA rating might not be a good measure for the sensitivity analysis because it ignores sign in measuring differences between two responses.

Limitations of this study are the following:

1. Only one loading case was considered in this study and it was not sufficient to evaluate biofidelity and find sources of errors of the GHBMC model.
2. Due to the difficulty to change an initial posture of the GHBMC model, variations in initial posture of the arms were not considered.

## VI. REFERENCES

- [1] Crandall JR, Bose D, Forman J, Untaroiu CD, Arregui-Dalmases C, Shaw, CG, Kerrigan JR, Human surrogates for injury biomechanics research, *Clin. Anat.*, 24(3):362–371, 2011.
- [2] Eppinger R, Marcus J, Morgan R, Development of Dummy and Injury Index for NHTSAs Thoracic Side Impact Protection Research Program, *SAE Technical Paper*, 840885, 1984.
- [3] Lizee E, Robin S, Song E, Bertholon N, Coz JYL, Besnault B, and Lavaste F, Development of a 3D finite element model of the human body, *Stapp Car Crash J*, 42:124–149, 1998.
- [4] Behr M, Arnoux PJ, Serre T, Bidal S, Kang HS, Thollon L, Cavallero C, Kayvantash K, Brunet C, A human model for road safety: from geometrical acquisition to model validation with Radioss, *Computer Methods in Biomechanics and Biomedical Engineering*, 6(4):263-273, 2003.
- [5] Documentation of Total Human Model for Safety (THUMS) AM50 Pedestrian/Occupant Model. Toyota Motor Corporation, 2010.
- [6] Robin S, Human Model for Safety—a joint effort towards the development of redefined human-like car-occupant models, *17th International Conference for the Enhanced Safety of Vehicles*, Amsterdam, 2001.
- [7] Iwamoto M, Kisanuki Y, Wantanabe I, Furusu K, Miki K, and Hasegawa J, Development of a finite element model of the Total Human Model for Safety (THUMS) and application to injury reconstruction, *International Research Council on the Biomechanics of Injury (IRCOBI)*, Munich Germany, 2002.
- [8] Shaw CG, Crandall JR, Butcher J, Biofidelity Evaluation of the THOR Advanced Frontal Crash Test Dummy, *IRCOBI Conference on the Biomechanics of Impact*, Montpellier France, 2000.
- [9] Shaw CG, Ash J, Lessley D, Sochor M., Carlos AD, Crandall JR. Side Impact PMHS Thoracic Response with Large Volume Airbag, Manuscript submitted for publication
- [10] LS-DYNA Keyword User's Manual, Version 971, Livermore Software Technology Corporation
- [11] Schneider LW, Robbins DH, Pflug MA, Snyder RG, Anthropometry of Motor Vehicle Occupants, Vol. 3. Specifications and Drawings. Report HS-806 717; UMTRI-83-53-2, UMTRI, 1983.
- [12] Eppinger RH, On the Development of a Deformation Measurement System and Its Application Toward Developing Mechanically Based Injury Indices, *Proceedings of the 33rd Stapp Car Crash Conference*, Warrendale, Pa: Society of Automotive Engineers. 21-28. SAE 892426., 1989.
- [13] David Lessley, Greg Shaw, Daniel Parent, Carlos Arregui-Dalmases, Matthew Kindig, Patrick Riley, Sergey Purtsezov, Mark Sochor, Thomas Gochenour, James Bolton, Damien Subit, Jeff Crandall, Whole-body response to pure lateral impact, *Stapp Car Crash Journal*, Arizona USA, Vol. 54., 2010.
- [14] Park G, Kim T, Ash J, Lessley D, Shaw CG and Crandall J, Evaluation of ES-2re dummy FE model under side impact sled tests with side airbag condition, Manuscript submitted for publication
- [15] Gehre C, Gades H, and Wernicke P, Objective rating of signals using test and simulation responses, *21<sup>st</sup> International Technical Conference on the Enhanced Safety of Vehicles Conference (ESV)*, Paper 09-0407, Germany, 2009.
- [16] Society of Automotive Engineers. SAE Surface Vehicle Information Report: Sign Convention for Vehicle Crash Testing – SAE J1733. 1994.
- [17] Society of Automotive Engineers, Surface Vehicle Recommended Practice J211-1 – Instrumentation for Impact Test – Part 1 – Electronic Instrumentation, Warrendale, PA. 2003.

- [18] Vavalle NA, Moreno DP, Rhyne AC, Stizel JD, and Gayzik FS, Lateral Impact Validation of a Geometrically Accurate Full Body Finite Element Model for Blunt Injury Prediction, *Annals of Biomedical Engineering*, 2012.
- [19] Beillas P, and Berthet F, Performance of a 50th percentile abdominal model for impact: effect of size and mass, *European Society of Biomechanics Conference*, 2012.
- [20] DeWit JA, and Cronin DS, Cervical spine segment finite element model for traumatic injury prediction, *J. Mech. Behav, Biomed. Mater*, 10:138–150, 2012.
- [21] Fice JB, Cronin DS, and Panzer MB, Cervical spine model to predict capsular ligament response in rear impact, *Ann. Biomed. Eng.*, 39:2152–2162, 2011.
- [22] Li Z, Kindig MW, Kerrigan JR, Untaroiu CD, Subit D, Crandall JR, and Kent RW, Rib fractures under anterior-posterior dynamic loads: experimental and finiteelement study, *J. Biomech.*, 43:228–234, 2010.
- [23] Li Z, Kindig MW, Subit D and Kent RW, Influence of mesh density, cortical thickness and material properties on human rib fracture prediction, *Med. Eng. Phys.*, 32, 998–1008, 2010.
- [24] Mao H, Zhang L, Jiang B, Genthikatti VV, Jin X, Zhu F, Makwana R, Gill A, Jandir G, Singh A, and Yang KH, Recent advances in developing finite element head model, *International Crashworthiness Conference*, Milan Italy, 2012.
- [25] Shin J, Yue N., and Untaroiu CD, A finite element model of the foot and ankle for automotive impact applications, *Ann. Biomed. Eng.*, 2012.